Computer Simulation of Catalytic Oxidation of Gaseous Ammonia in Bubbling Fluidized Bed

P. Kannan*, A. Al Shoaibi, and C. Srinivasakannan
Department of Chemical Engineering, The Petroleum Institute,
P.O. Box 2533, Abu Dhabi, UAE

Original scientific paper
Received: October 24, 2012
Accepted: May 2, 2013

Catalytic conversion of ammonia in bubbling fluidized bed has been simulated using three different hydrodynamic models: (a) Kunii and Levenspiel model, (b) Simple two-phase model, and (c) Dynamic two-phase model. The basic differences between the models lie in the assumptions and mass transfer correlations used to describe the hydrodynamics of the fluidized bed. This study compares the predictions of the performance of a fluidized bed reactor by different models, comparing with experimental data of ammonia oxidation using metal oxide catalysts. The predictions from all the models compared well with the experimental data within acceptable levels of error. The variations among the models were found to be insignificant. However, simulation of the model to assess the effect of different hydrodynamic parameters, including gas velocity, bed diameter and particle size, and bed density on conversion showed significant variation among the models.

Key words:
Catalytic oxidation of ammonia, fluidized bed, simulation

1. Introduction

For long, ammonia has been branded as a harmful acid pollutant causing irreversible damage to the environment. Unlike other pollutants like nitrogen oxides (NO_x) and sulphur oxides (SO_x), ammonia causes acidification to the environment in a more complex and indirect way. The sequence of reactions between ammonia and acidic aerosols followed with microorganisms to form acidic HNO_3 has been well documented in the literature.[1,2] The sources of ammonia could be traced to various industries, including fertilizer manufacturing industry, coke manufacture, fossil fuel combustion, and biomass gasification. Moreover, ammonia is not only emitted by direct sources (process) but also through indirect means such as control technologies of other pollutants, especially nitrogen oxides (NO_x). Selective catalytic reduction (SCR) is one of the main technologies employed for controlling NO_x emissions. A significant amount of ammonia is added to the SCR process to convert NO_x to nitrogen according to the reaction: $NH_3 + NO + 1/4\ O_2 \rightarrow N_2 + 3/2\ H_2O$. However, depending on the extent of the reaction, excess ammonia may exit the process along with the effluent, a condition referred to as "ammonia slip".[3] Subsequently, an ammonia removal or conversion process has to be installed as a downstream operation in addition to the SCR process to curtail ammonia being released as a pollutant.[4,5]

Selective catalytic oxidation (SCO) of ammonia is a relatively new technology that converts ammonia to nitrogen and water in the presence of catalysts. Besides providing an efficient and stable operation, it can be selectively used to enhance pure nitrogen production from air and ammonia suitable for various applications.[6] The following reactions depict the chemistry of SCO of ammonia:

$$2\ NH_3 + 3/2\ O_2 \rightarrow N_2 + 3\ H_2O + 632\ kJ \quad (1)$$

$$2\ NH_3 + 2\ O_2 \rightarrow N_2O + 3\ H_2O + 552\ kJ \quad (2)$$

$$2\ NH_3 + 5/2\ O_2 \rightarrow 2\ NO + 3\ H_2O + 451\ kJ \quad (3)$$

While elevated process temperatures (750 – 900 °C) favor high production of nitrogen oxides (Reactions (2) and (3)), low temperature conditions (< 500 °C) result in the formation of all nitrogen compounds in varying proportions depending on the catalyst. SCO focuses on maximizing the composition of nitrogen by limiting Reactions (2) and (3) using various metal and metal oxide catalysts. A detailed review discussing the effect of catalyst performance, temperature, and O_2/NH_3 ratio has been presented in the literature.[7]

Typically a plant processing large throughput utilizes fluidized beds due to the advantages such as excellent mixing characteristics,[8] operating flexibility,[9] and ease of solids handling[10] that lead to a better overall conversion efficiency. Although it is

*Corresponding Author: Email: pkannan@pi.ac.ae, Off: +971-26020926, Fax: +971-26075200

marked by relatively lower conversion than fixed bed for a given amount of catalyst, fluidized bed has been the preferred choice of reactor for most of the heterogeneous gas-solid catalytic reactions owing to uniform reactor temperature and ease in operation. Examples of industrial applications of such reactors include catalytic cracking of hydrocarbons; coal gasification; ore roasting; and synthesis reactions such as Fischer-Tropsch synthesis, polyethylene production, and maleic anhydride production.[11]

In order to predict performance and scale-up of fluidized bed reactors, it is imperative to develop a model that would account for the conversion of the reactants, encompassing all the reactor conditions. However, due to a certain degree of uncertainty in predicting the performance of the fluidized bed, its application to complex reactions has been restricted. One of the main causes of uncertainties is due to the unaccountability of non-uniformities in gas distribution in the form of bubbles and channels.[12] Such anomalies in bed characteristics strongly question any predictions of system behavior unless they are accurately described and captured by the mathematical model. Most of the fluidized bed models have been developed from the principles of two-phase fluidization, originally developed by Toomey and Johnstone.[13] Since then, many researchers have employed similar or modified versions of the model to investigate different reaction systems, including production of maleic anhydride (MAN) by the catalytic oxidation of *n*-butane,[14] and ammoxidation of propylene.[15] This study aims to test both the simple and dynamic two-phase hydrodynamic models against a relatively unexplored reaction system, selective catalytic oxidation of ammonia using a fluidized bed. The bed operates in bubbling regime wherein the reactants, ammonia and oxygen enters the bed from the bottom and flows upwards. Products along with unconverted reactants exit the reactor at the top, which may undergo different separation operations for purification. Conversion predicted by both models is compared and validated against experimental data reported by Massimilla.[12] Results of the present work are expected to shed more light on improving the predictions of ammonia conversion under different process conditions.

2. Model development

2.1. Hydrodynamics

Two most generic two-phase bubbling bed models along with the three-phase Kunii-Levenspiel model were utilized to simulate the SCO reaction system in bubbling fluidized bed. Reactant gas enters the bottom of the bed and flows up the reactor partly in the emulsion phase and the rest in the form of bubbles. As the bubbles rise through the bed, mass transfer between the phases facilitates transfer of reactants and products in both directions. The reactants diffuse from bubble phase to the emulsion phase where the presence of catalyst (solid particles), promotes the reaction. The rate at which the reactants and products transfer in and out of the bubble affects the conversion, as does the duration of the bubble in the bed.[11] The simple two-phase hydrodynamic model assumes that all gas in excess of minimum fluidization passes through the bed as solid-free bubbles, and that the emulsion phase remains at minimum fluidization conditions all the time. However, it has been verified experimentally and theoretically in works[16–20] that there remains a dynamic distribution of particles between the bubble and emulsion phase, and that the latter possesses excess gas at higher superficial gas velocities. Dynamic two-phase model attempts to capture these observations with appropriate modification to the semi-empirical equations, accounting the reaction simultaneously in both phases. Kunii & Levenspiel model considers a three-phase regime consisting of bubble, cloud and emulsion wherein reaction occurs only in the dense phase with continuous interchange of reactants and products.

Kunii-Levenspiel model

Since most of the catalytic reactions in dense bubbling fluidized beds use fine Geldart A solids that have a very small minimum fluidization velocity, Kunii and Levenspiel assumed that all the fed gas passes through the bed as bubbles, and flow through the emulsion phase is negligible.[16] This three-phase bubbling bed model was developed under the following assumptions:

1. Bubbles are all of single size.

2. Solids in the emulsion phase flow smoothly downward, essentially in plug flow.

3. Emulsion phase exists at minimum fluidizing conditions. The gas occupies the same void fraction in this phase as it had in the entire bed at minimum fluidization point.

4. In the wake, the concentration of solids is equal to the concentration of solid in the emulsion phase, and therefore the gaseous void fraction in the wake is also the same as in the emulsion phase.

The exchange of gases between various phases along with the reaction is depicted in Fig. 1. Details of model description and development can be found elsewhere.[16]

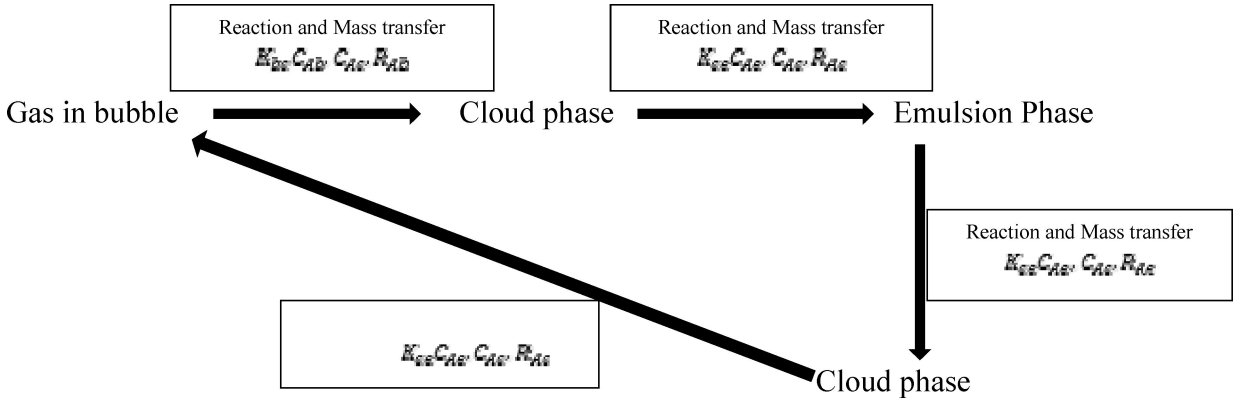

Fig. 1 – *Mass transfer in bubbling fluidized bed as described by K-L model*

Simple two-phase model

The simple two-phase bubbling bed model has been widely tested for various reaction systems and the common consensus is that it provides only approximate predictions of the performance of fluidized bed. Nevertheless, it has been considered in this study in order to enhance a better understanding and comparison with other flow models.

Assumptions involved:

1. Fluidized bed reactor consists of two phases: Bubble Phase and Emulsion Phase
2. All gases in excess of the minimum fluidization velocity flow through the bed as bubbles
3. Emulsion Phase remains stagnant at the minimum fluidization conditions ($U_e = U_{mf}$)
4. Bubbles are solid-free with reaction occurring only in the emulsion phase.

The interchange of reactants and products of the two-phase model is depicted in Fig. 2.

The solution of the two differential equations representing the mole balance in bubble and emulsion phases yields an expression to calculate average reactant concentration, and hence the exit conversion. Furthermore, this expression can be used to estimate conversion for different solid particle size, superficial velocity, reactor diameter, and height.

Dynamic two-phase model

The actual flow structure in the fluidized beds is more complicated than that described in the simple two-phase model. In a real fluidized bed, the concentration of particles in the emulsion phase can be less than that at minimum fluidization, and the bubbles can contain various amounts of particles. Therefore, this model considers the progress of the reaction in both the bubble and emulsion phases.

Assumptions involved:

1. Fluidized bed reactor consists of two phases: Bubble Phase and Emulsion Phase[21]
2. All gases in excess of the minimum fluidization velocity flow through the bed as bubbles
3. Emulsion Phase remains stagnant at the minimum fluidization conditions ($U_e = U_{mf}$).
4. Bubbles are not solid-free with reaction occurring both in bubble and emulsion phase.

Since the reaction takes place in both the bubble and emulsion phase, reaction rate is calculated in both the phases depending on the local reactant concentrations. Equations describing the diffusion and reaction process are similar to the simple two-phase model except for an additional reaction term in the bubble-phase mole-balance equation. The initial conditions for the two differential equations are taken such that the initial concentration in both the phases is equal to the entering reactant concentration.

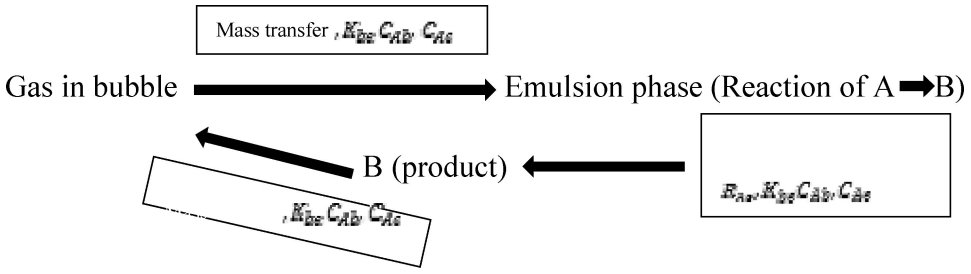

Fig. 2 – *Mass transfer and reaction in a simple two phase fluidized bed model*

Table 1 – *Summary of state equations and mass transfer correlations used in this study*

	K-L model	Simple two-phase model	Dynamic two-Phase model
Mole balance for Species A in different phases	$\frac{dC_{Ab}}{dz}=-k_bC_{Ab}-k_{bc}\left(C_{Ab}-C_{Ac}\right)$ $k_{bc}(C_{Ab}-C_{Ac})=k_cC_{Ac}+k_{ce}(C_{Ac}-C_{Ae})$ $k_{ce}(C_{Ac}-C_{Ae})=k_eC_{Ae}$	$\frac{\mathrm{d}C_{Ab}}{\mathrm{d}z}=-\frac{k_{be}(C_{Ab}-C_{Ae})}{U_b}$ $\frac{\mathrm{d}C_{Ae}}{\mathrm{d}z}=\frac{k_{be}\delta(C_{Ab}-C_{Ae})+R_{Ae}(1-\delta)(1-\varepsilon_{mf})}{U_{mf}(1-\delta)}$	$\frac{\mathrm{d}C_{Ab}}{\mathrm{d}z}=\frac{R_{Ab}(1-\varepsilon_b)(1-\delta)-k_{Be}(C_{Ab}-C_{Ae})}{U_b}$ $\frac{\mathrm{d}C_{Ae}}{\mathrm{d}z}=\frac{R_{Ae}(1-\varepsilon_e)(1-\delta)-k_{Be}(C_{Ab}-C_{Ae})}{U_e(1-\delta)}$
Overall Concentration		$C_{Avg}=\frac{\delta u_bC_{Ab}+(1-\delta)u_{mf}C_{Ae}}{u_0}$.	$C_{Avg}=\frac{u_{mf}(1-\delta)}{u_0}C_{Ae}+\frac{u_b\delta}{u_0}C_{Ab}$
Rate Equation	$R_{Ab}=-\gamma_bk_{cat}C_{Ab}$ $R_{Ac}=-\gamma_ck_{cat}C_{ac}$ $R_{Ae}=-\gamma_ek_{cat}C_{Ae}$	$R_{Ae}=-k_{cat}C_{Ae}$	$R_{Ab}=-k_{cat}C_{Ab}$ $R_{Ae}=-k_{cat}C_{Ae}$
Bubble fraction	$\delta=\frac{U_0-U_{mf}}{U_b-U_{mf}(1+\alpha)}$	$\delta=\frac{u_0-u_{mf}}{u_b-u_{mf}}$	$\delta=\frac{u_0-u_{mf}}{u_b-u_{mf}}$
Bubble diameter	$d_b=d_{bm}-\left(d_{bm}-d_{bo}\right)e^{\frac{-0.3H}{d_t}}$ $d_{bo}=0.00376\,(u_0-u_{mf})^2$ $d_{bm}=0.65\,[A(u_0-u_{mf})]^{0.4}$	$d_b=d_{bm}-\left(d_{bm}-d_{bo}\right)e^{\frac{-0.3H}{d_t}}$ $d_{bo}=0.00376\,(u_0-u_{mf})^2$ $d_{bm}=0.65\,[A(u_0-u_{mf})]^{0.4}$	$d_b=d_{bm}-\left(d_{bm}-d_{bo}\right)e^{\frac{-0.3H}{d_t}}$ $d_{bo}=0.00376\,(u_0-u_{mf})^2$ $d_{bm}=0.65\,[A(u_0-u_{mf})]^{0.4}$
Minimum fluidization Velocity	$u_{mf}=\frac{\left(\varphi d_s\right)^2}{150\mu_g}\left[g\left(\rho_s-\rho_g\right)\right]\frac{\varepsilon_{mf}^3}{(1-\varepsilon_{mf})}$	$u_{mf}=\frac{\left(\varphi d_s\right)^2}{150\mu_g}\left[g\left(\rho_s-\rho_g\right)\right]\frac{\varepsilon_{mf}^3}{(1-\varepsilon_{mf})}$	$u_{mf}=\frac{\left(\varphi d_s\right)^2}{150\mu_g}\left[g\left(\rho_s-\rho_g\right)\right]\frac{\varepsilon_{mf}^3}{(1-\varepsilon_{mf})}$
Bubble Velocity	$u_b=u_o-u_{mf}+0.711(gd_b)^{1/2}$	$u_b=u_o-u_{mf}+0.711(gd_b)^{1/2}$	$u_b=u_o-u_{mf}+0.711(gd_b)^{1/2}$
Emulsion velocity			$u_e=\frac{u_0-\delta u_b}{1-\delta}$
Gas Interchange coefficient	$k_{bc}=4.5\left(\frac{u_{mf}}{d_b}\right)+5.85\left(\frac{D_{AB}^{0.5}g^{0.25}}{d_b^{1.25}}\right)$ $k_{ce}=6.78\left(\frac{\varepsilon_{mf}D_{AB}u_b}{d_b^3}\right)^{0.5}$	$k_{be}=\left(\frac{1}{k_{bc}}+\frac{1}{k_{ce}}\right)^{-1}$ $k_{bc}=4.5\left(\frac{u_{mf}}{d_b}\right)+5.85\left(\frac{D_{AB}^{0.5}g^{0.25}}{d_b^{1.25}}\right)$ $k_{ce}=6.78\left(\frac{\varepsilon_{mf}D_{AB}u_b}{d_b^3}\right)^{0.5}$	$k_{be}=\left(\frac{1}{k_{bc}}+\frac{1}{k_{ce}}\right)^{-1}$ $k_{bc}=4.5\left(\frac{u_{mf}}{d_b}\right)+5.85\left(\frac{D_{AB}^{0.5}g^{0.25}}{d_b^{1.25}}\right)$ $k_{ce}=6.78\left(\frac{\varepsilon_{mf}D_{AB}u_b}{d_b^3}\right)^{0.5}$
Average Emulsion Voidage	–	–	$\varepsilon_e=\varepsilon_{mf}+0.00061\exp\left(-\frac{u_0-u_{mf}}{0.262}\right)$
Average Bubble voidage	–	–	$\varepsilon_b=0.784-0.139\exp\left(-\frac{u_0-u_{mf}}{0.272}\right)$
Average bed voidage	–	$\varepsilon=(1-\delta)\varepsilon_{mf}+\delta$	$\varepsilon=(1-\delta)\varepsilon_e+\delta\varepsilon_b$
Voidage at minimum Flu. Conditions	$\varepsilon_{mf}=0.586\varphi^{-0.72}(\frac{\mu_g^2}{\rho_g\left(\rho_s-\rho_g\right)gd_s^3})^{0.029}\left(\frac{R_g}{R_S}\right)^{0.021}$	$\varepsilon_{mf}=0.586\varphi^{-0.72}(\frac{\mu_g^2}{\rho_g\left(\rho_s-\rho_g\right)gd_s^3})^{0.029}\left(\frac{R_g}{R_S}\right)^{0.021}$	$\varepsilon_{mf}=0.586\varphi^{-0.72}(\frac{\mu_g^2}{\rho_g\left(\rho_s-\rho_g\right)gd_s^3})^{0.029}\left(\frac{R_g}{R_S}\right)^{0.021}$
Terminal veloctiy	$u_t=\left(\frac{1.78.10^{-2}[g\left(\rho_s-\rho_g\right)]^2}{\rho_g\mu_g}\right)^{\frac{1}{3}}\left(d_s\right)$ $0.4<Re_s<500$	$u_t=\left(\frac{1.78.10^{-2}[g\left(\rho_s-\rho_g\right)]^2}{\rho_g\mu_g}\right)^{\frac{1}{3}}\left(d_s\right)$ $0.4<Re_s<500$	$u_t=\left(\frac{1.78.10^{-2}[g\left(\rho_s-\rho_g\right)]^2}{\rho_g\mu_g}\right)^{\frac{1}{3}}\left(d_s\right)$ $0.4<Re_s<500$
Partitioning of catalyst	$\gamma_b=0.001-0.01$ $\gamma_c=(1-\varepsilon_{mf})\left[\frac{3\left(\frac{u_{mf}}{\varepsilon_{mf}}\right)}{u_b-\left(\frac{u_{mf}}{\varepsilon_{mf}}\right)}+\alpha\right]$ $\gamma_e=(1-\varepsilon_{mf})\left[\frac{1-\varepsilon}{\varepsilon}\right]-\gamma_c-\gamma_b$	–	–

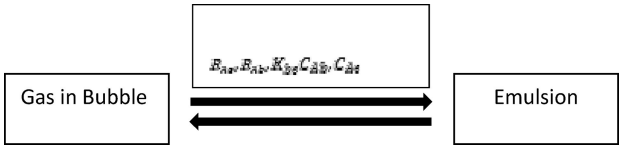

Fig. 3 – *Mass transfer in fluidized bed as depicted by dynamic two-phase model*

The corresponding model equations for each of the models, along with mass transfer correlations are listed in Table 1. The variation in the bubble fraction in the bed among the models can be noted from the list of equations.

2.2. Kinetics

Johnstone et al[12] proposed that the oxidation of ammonia over the magnesia-bismuth oxides on alumina spheres follows a pseudo-first-order reaction, and the solution of differential equation representing the mass balance for plug flow reactor and reaction of first-order solution yields

$$\ln(1-\alpha) = -k_{cat} \cdot \tau \tag{4}$$

where α s the overall fraction of ammonia oxidized, τ s the reciprocal of space velocity expressed as volume of catalyst particles per unit of volumetric gas flow rate, and k_{cat} is the reaction rate constant. Using fixed bed reactor under similar experimental conditions, the average value of rate constant was reported as 0.0858 s^{-1}.

3. Simulation

K-L model was simulated in MATLAB and the two-phase model equations were solved in Polymath using the input parameters listed in Table 2.

Table 2 – *Summary of input conditions used for simulation*

Pressure	1.125	bar
Temperature	523	K
Reactor diameter	11.4	cm
Volumetric flow rate	818	$cm^3\ s^{-1}$
Initial Reactant Composition	10% NH_3 – 90% O_2	
Particle diameter (d_p)	105	μm
Particle density (ρ_p)	2.06	g cm^{-3}
Height of unexpanded bed	38.9	cm
k_{cat} (per vol of solid catalyst)	0.0858	s^{-1}
Gas density (ρ_g)	7.85E-04	g cm^{-3}
Viscosity at 523 k	2.98E-04	g $cm^{-1}\ s^{-1}$
Gas diffusion coefficient (D_{ab})	0.618	$cm^2\ s^{-1}$

The differential equation that accounts for the changes in the concentration of reactant ammonia with respect to bed height in the two-phase models is solved simultaneously using Stiff algorithm available in Polymath. The three models predictions were compared with the experimental data for ammonia oxidation reported by Massimilla et al.[12] Further, all the three models were used for investigating the effects of various hydrodynamic parameters on the conversion efficiency of catalytic oxidation of ammonia.

4. Results and discussion

4.1. Model validation

Experimental data on catalytic oxidation of ammonia in bubbling fluidized bed reactor is very limited in literature. It could be noticed from Table 1 that the equations used to calculate fluidization parameters are similar for all hydrodynamic models. However, the mass transfer and reaction rate equations considered by each model differs and therefore, it could be expected that the resulting exit conversion may differ among each model. The test case simulation was performed at a gas velocity of 8.01 cm s^{-1} in an 11.4 cm reactor diameter with 105 μm particle size and 4 kg catalyst weight at 523 K; see Table 2 for complete specifications on process conditions. The computed values of fluidization parameters along with conversion from all the three models are presented in Table 3. It is evident that each model differs only in the way the overall mass transfer coefficient and reactions rates are defined and calculated. Simulation results are found to be in good agreement with the experimental data for SCO of ammonia reported by Massimilla and Johnstone[12] who reported an exit conversion of 15 % for the same base conditions while that of simple, dynamic and K-L models reported 17.18 %, 18.39 % and 19.63 % respectively. In the two-phase model, the reaction is presumed to occur only in the emulsion phase since the bubbles are solid-free, whereas in the dynamic phase the reaction takes place in the bubble phase as well. However, the K-L model accounts for mass transfer and reaction in bubble, cloud and emulsion phases estimating an overall conversion higher than the two-phase models.

The conversion profile of ammonia along the length of the reactor predicted by various models is illustrated in Fig. 4. It should be noted that all the models assumes uniform radial concentration profile in the bed, which is also evident in the mole balance equations. Normalized axial length was calculated by dividing the axial length (z) with the final expanded bed height (H). The composition of the gas leaving the bed is calculated based on the

Table 3 – *Comparison between K-L and two phase models for SCO of ammonia.*

Model Parameters	K-L Model	Simple two phase model	Dynamic two phase model	Units
Porosity at minimum fluidization, ε_{mf}	0.657	0.657	0.657	
Min. fluidization velocity, U_{mf}	1.48	1.48	1.48	cm s^{-1}
Terminal velocity, U_t	71.05	71.05	71.05	cm s^{-1}
Bubble size, d_b	4.86	4.86	4.86	cm
Velocity of Bubble Rise, U_b	55.63	55.62	55.62	cm s^{-1}
Bubble fraction, δ	0.121	0.121	0.121	
Volume of catalyst in bubbles, clouds, and emulsion, γ_b, γ_c, γ_e	0.01, 0.1806, 2.27			
Bubble cloud mass transfer coefficient, K_{bc}	4.93	4.93	4.93	s^{-1}
Cloud-emulsion mass transfer coefficient, K_{ce}	2.99	2.82	2.82	s^{-1}
Overall transport co-efficient for a first order reaction, K_r	2.241			
Overall Exit Conversion (X)	0.1963	0.1718	0.1839	
Specific reaction rate in bubble phase, k_b	0.000858			Per unit vol of bubble
Specific reaction rate in cloud phase, k_c	0.015			Per unit vol of bubble
Specific reaction rate in emulsion phase, k_e	0.196			Per unit vol of bubble
Height of expanded bed	63.23	63.13	63.13	cm

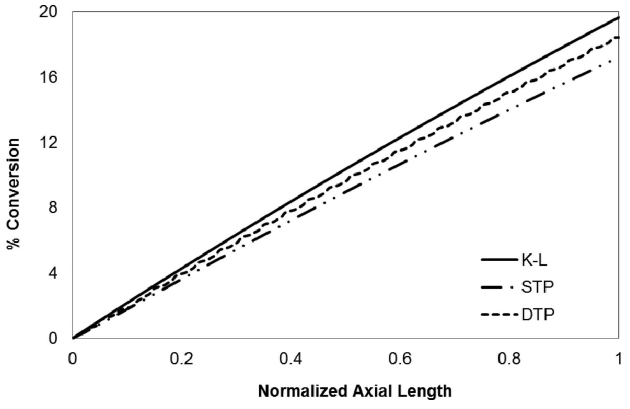

Fig. 4 – *Axial conversion profile of conversion for various models*

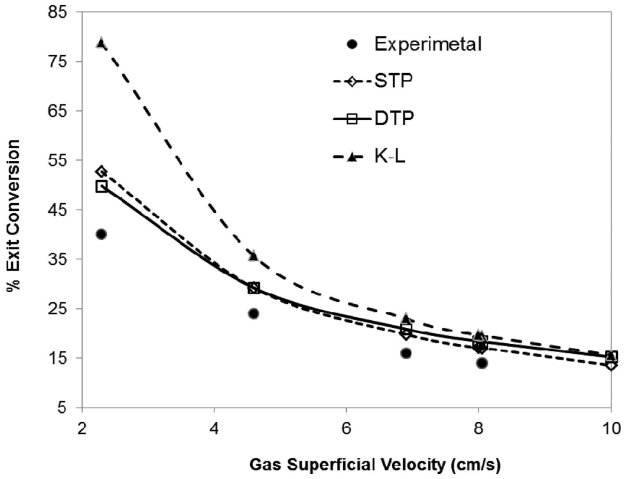

Fig. 5 – *Overall ammonia conversion as a function of superficial gas velocity*

average of composition of all the phases involved in the flow model.

Detailed comparison of model predictions with additional experimental data is presented in Section 4.2.1.

4.2. Influence of hydrodynamic parameters

4.2.1. Effect of superficial gas velocity

Fig. 5 shows the effect of fluidization gas velocity on overall conversion of ammonia calculated at the exit of the bed. Predictions from all three models have been compared with experimental data reported by Masimilla et al.[12] All other system parameters, including temperature, particle diameter, and bed diameter were kept constant in all simulations as that of the base case model. It is evident from Fig. 5 that an increase in gas velocity exponentially decreases the conversion and at low gas velocities, the conversion remains high due to the fact that the behavior of the bed remains close to fixed-bed conditions. The effect of gas velocity

seems to be very significant at lower values (indicated by the steepness of the curves) while at higher gas velocities it reaches an asymptote. The increase in gas velocity is expected to increase the bed height at expanded conditions due to increase in the bubble fraction in the bed which may contribute to the increase in conversion. However, it would lead to an increased bubble size and hence a higher bubble rise velocity and thereby the reduction in gas residence time in the bed, the cumulative effect of which results in the reduction of overall conversion with increase in gas velocity. Furthermore, at lower gas velocities, the volume of gases flowing through the dense phase is higher than the gas exiting through the bubbles. Since the dense phase is more concentrated with catalyst particles, the rate of reaction is higher in the emulsion than anywhere in the bed. The combined effect of gas velocity and mass transfer coefficient is better understood through the definition of the number of transfer units (NTU) given by Mostoufi et al.[14]

$$NTU = {k_{be}H}/{U_o} \tag{1}$$

The mass transfer from bubble-to-cloud-to-emulsion significantly affects the concentration profiles in the fluidized bed. It can be observed for the K-L model that the number of transfer units decreases significantly with increasing gas velocity indicating that the overall conversion would tend to decrease, as could be noticed in Fig. 6.

Under the range of superficial gas velocity investigated, it was found that the emulsion velocity is not much different from the minimum fluidization velocity for all cases. This translates to similar mass transfer coefficient and number of transfer units for both the simple two-phase model and the dynamic model as shown in Fig. 6. Furthermore, at elevated gas velocities, it can be inferred that the predictions of even the K-L model approaches that of the two-phase models implying that the overall conversion tends to be solely in the bubbles rather than in the cloud or emulsion. The conversion rate is governed by the reaction kinetics in the emulsion phase for the simple two-phase while by both the phases for dynamic two-phase model.

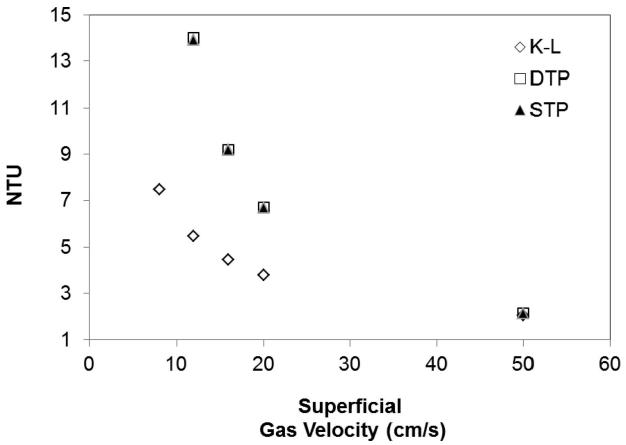

Fig. 6 – *Variation of the number of transfer units (NTU) with superficial gas velocity*

4.2.2. Effect of bed diameter

Fig. 7 shows the effect of bed diameter on the overall exit conversion of ammonia while the other simulation parameters held constant as that of the base case simulation. It is well-known that the rate at which the reactants and products transfer in and out of the bubbles and the residence time of bubble in the bed affects conversion. It can be noticed from Fig. 6 that the conversion decreases with increase in bed diameter for all the hydrodynamic models. An increase in the bed diameter at a constant volumetric flow rate of the gas phase is expected to reduce the effective fluidization velocity, resulting in lower bed height, and lower fraction of bubble in the bed leading to a drop in conversion. As expected, conversion predicted by K-L model is higher than the dynamic two-phase model, which is higher than the simple two-phase model.

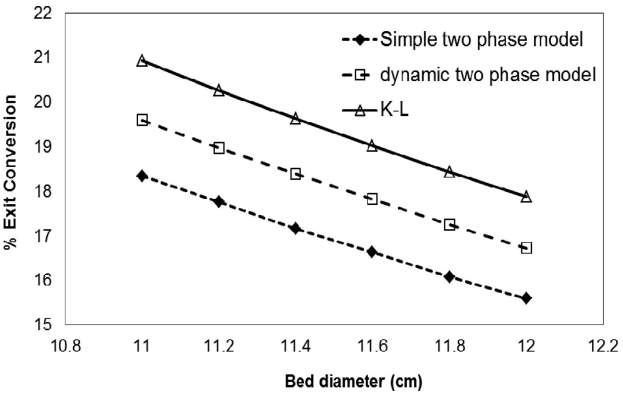

Fig. 7 – *Overall ammonia conversion as a function of bed diameter*

4.2.3. Effect of particle size and particle density

Fig. 8 shows the effect of bed particle size on conversion efficiency with the other simulation parameters same as the base case simulation and at a reaction temperature of 523 K. It should be noted that the bed particle and its properties represent the actual catalyst used in experimental study. It can be noticed that conversion increases with increase in particle diameter. It is worth mentioning that any change in particle size would increase bed density; however particle density would remain unchanged. As the particle size increases with other parameters being constant, the bubble fraction in the bed and

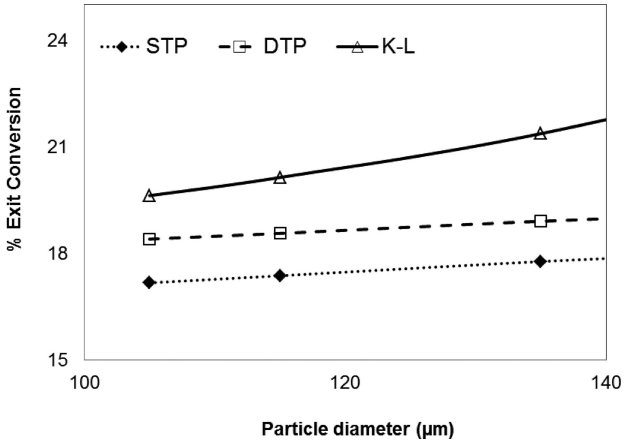

Fig. 8 – *Overall ammonia conversion as a function of particle diameter*

the bed height decreases, both of which would contribute to lower conversion. However, at the same time, there is also a significant decrease in bubble velocity which consequently increases residence time and increases conversion. The decrease in bubble velocity on increasing particle diameter could be attributed to the higher minimum fluidization velocity at large particle sizes.

The effect of catalyst particle density on ammonia conversion efficiency follows the same trend as particle size and has been illustrated in Fig. 9. At lower catalyst densities, the agreement between the three model predictions is better than at conditions of higher densities. At higher densities, the overall conversion tends to be closer to that of emulsion because of the higher concentration of catalyst particles in the dense/cloud phase rather than the bubble phase. Moreover, comparing the values of DTP and K-L models, it can be inferred that K-L model predicts higher conversion for a given particle density, possibly indicating the occurrence of reaction in the cloud phase (immediately outside the bubble) rather than in the emulsion.

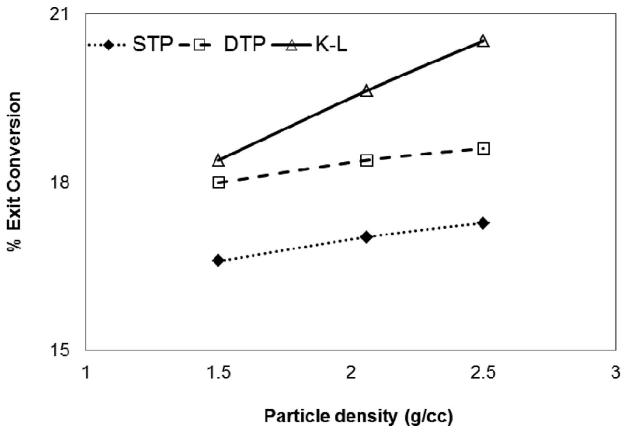

Fig. 9 – *Overall ammonia conversion as a function of particle density*

Conclusions

This study focuses on modeling the catalytic conversion of ammonia using bubbling fluidized bed by three different and widely used hydrodynamic models. The flow models predict the overall conversion of ammonia using mathematical equations describing mass transfer and reaction rates. The basic difference between the three hydrodynamic models lies in the way the fluidized bed is described. Comparison between the predictions from the proposed models with the limited experimental data available for the reaction system proved satisfactory. After validation, the three models were tested against various hydrodynamic conditions like superficial gas velocity, bed diameter, particle size, and bed density. Although the three models showed deviations from each other, the qualitative trend on each of the parametric effects were similar and in good agreement with theoretical predictions. The present model can be extended to investigate any first-order gas-solid catalytic reaction system in fluidized bed.

ACKNOWLEDGEMENT

The authors would like to extend their sincere appreciation to Borouge Plastics for their financial support.

List of symbols

U_{mf} – minimum fluidization velocity, m s^{-1}
U_e – emulsion velocity, m s^{-1}
U_o – superficial gas velocity, m s^{-1}
U_{br} – bubble rise velocty, m s^{-1}
U_t – terminal velocity, m s^{-1}
ε_{mf} – voidage at minimum fluidization
ε – average bed voidage
ε_b – average bubble voidage
ε_e – average emulsion voidage
α – overall conversion of ammonia
D_{AB} – gas diffusion coefficient, m^2 s^{-1}
NTU – number of mass transfer units
τ – reciprocal of space velocity
H – height of unexpanded bed m
z – distance above the distributor plate m
δ – bubble fraction in fluidized bed
γ_b – distribution of catalyst in bubble phase
γ_c – distribution of catalyst in cloud phase
γ_e – distribution of catalyst in emulsion phase
C_{avg} – average concentration, mol L^{-1}
d_b – bubble diameter m
d_{bm} – maximum bubble diameter m
d_t – bed diameter m

d_s – diameter of solid particles m
k_{cat} – overall reaction rate constant, s^{-1}
k_b – reaction rate constant in bubble phase, s^{-1}
k_c – reaction rate constant in cloud phase, s^{-1}
k_e – reaction rate constant in emulsion phase, s^{-1}
R_{Ab} – reaction rate of species A in bubble phase, mol g^{-1} s^{-1}
R_{Ac} – reaction rate of species A in cloud phase, mol g^{-1} s^{-1}
R_{Ae} – reaction rate of species A in emulsion phase, mol g^{-1} s^{-1}
k_{be} – bubble-to-emulsion gas interchange coefficient, s^{-1}
k_{bc} – bubble-to-cloud gas interchange coefficient, s^{-1}
k_{ce} – emulsion-to-cloud gas interchange coefficient, s^{-1}
μ_g – viscosity of gas Pa s
g – acceleration due to gravity, m s^{-2}
ρ_s – density of solid particles, kg m^{-3}
ρ_g – density of gas, kg m^{-3}
Re_s – Reynolds number

References

1. *Buijsman, E., Asman, W.,* Chemisch Magazine **12** (1983) 654.
2. *Frantzen, A. J., Adolphs, R., Schipper, W.,* Lucht en Omgeving **10** (1985) 132**.**
3. *Misenheimer, D., Warn, T., Zelmanowitz, S.,* Document No. EPA/600/7–87/001 (1987) U.S. Environmental Protection Agency, Air and Energy Engineering Research Laboratory,
4. *Amblard, M., Burch, R., Southward, B. W. L.,* Appl. Catal., B **22** (1999) 159.
5. *Biermann, J. J. P., Ph. D. Thesis* (1990) University of Twente: Twente, The Netherlands
6. *Gang, L., Ph. D. Thesis* (2002) Technische Universiteit Eindhoven: The Netherlands
7. *II'Chenko, N. I.,* Russ. Chem. Rev. **45** (1976) 1119.
8. *Sadaka, S. S., Ghaly A. E., Sabbah M. A.,* Biomass Bioenergy **22** (2002) 439.
9. *Arena, U., Zaccariello L., Mastellone M. L.,* Waste Manage **29** (2009)783.
10. *Mitta, N. R., Ferrer-Nadal, S., Lazovic, A. M., Parales, J. F., Velo, E., Puigjaner, L.,* Computer Aided Chemical Engineering, Elsevier, (2006).
11. *Kunii, D., Levenspiel, O.,* Fluidization Engineering, Butterworth-Heinemann, Boston, MA (1991).
12. *Massimilla, L., Johnstone, H. F.,* Chem. Eng. Sci. **16** (1961) 105.
13. *Toomey, R. D., Johnstone, H. F.,* Chem. Eng. Prog. **48** (1952) 220.
14. *Mostoufi, N., Cui, H., Chaouki, J.,* Ind. Eng. Chem. Res. **40** (2001) 5526.
15. *Ikeda, Y., Kagaku, K.,* Fluidization Engineering, Elsevier, Fukui City, Japan, 1970.
16. *Aoyagi, M., Kunii, D.,* Chem. Eng. Commun. **1** (1974) 191.
17. *Chaouki, J., Gonzalez, A., Guy, C., Klvana, D.,* Chem. Eng. Sci. **54** (1999) 2039.
18. *Batchelor, G. K., Nitsche, J. M.,* J. Fluid Mech. **278** (1994) 63.
19. *Gilbertson, M. A., Yates, J. G.,* J. Fluid Mech. **323** (1996) 377.
20. *Abrahamson, A. R., Geldart, D.,* Powder Technol. **26** (1980) 47.
21. *Werther, J.,* Chem. Eng. Sci. **47** (1992) 2457.